Structural properties, phase transition and electronic structure of InP and ZnS compound: Density-functional theory LDA, GGA, mbj-GGA calculations

Kh. Kabita[1], B. Indrajit sharma[2*], R. K. Brojen Singh[3] and R. K. Thapa[4]

[1](Department of Physics, Jiri College, Imphal East-795116, Manipur, India)
[2*](Department of Physics, Assam University Silchar, Silchar-788011, India)
[3](School of Computational and Integrative Sciences, JNU, New Delhi-110067, India)
[4](Department of Physics, Mizoram University, Tanhril, Aizawl-796 009, India)
Corresponding Author: B. Indrajit Sharma

Abstract: *The structural properties, phase transition and electronic structure of a semiconductor from the group III-V and II-VI compound are investigated to study their typical characteristics. We investigate the structural stability, phase transition under pressure and electronic structure with density functional theory (DFT) using full-potential linearized augmented plane wave (FP-LAPW) within the local-density approximation (LDA), generalized-gradient approximation (GGA) and modified Becke-Johnson generalized-gradient approximation (mbj-GGA). The present calculated structure parameters are in good agreement with the available experimental and theoretical data. The structural transition pressure of InP (zinc-blende to rock-salt structure) occurs at 6.07 GPa pressure with LDA and 9.3 GPa pressure with GGA method. The volume decreases 16.45% at the transition. The electronic structure calculation with mbj-GGA method gives better results as compared to the other LDA, GGA methods. Band diagram of InP (zinc-blende phase) shows a direct band gap of 1.31eV, and metallic in the rock-salt phase. Whereas, ZnS is a direct band gap of 3.5 eV in its zinc-blende phase and it is an indirect compound in rock-salt structure.*

Keywords: *Structure optimization, Phase transition, Electronic structure, Density functional theory*

I. Introduction

Gallium Phosphide, Gallium Arsenide, Indium Arsenide, Indium Phosphide (group III-V compound); Zinc Sulphide, Cadmium Telluride, Zinc Selenide (group II-VI compound compound) are some of the extensively studied compound semiconductors because of their useful physical, electro-optical and other distinctive properties. These materials are utilized for device applications such as top junction solar cells and multi-junction solar cell system in the electronics-telecommunication industries, and the military science [1-5]. It is, therefore essential for thorough investigations on their structural and electronic properties. In the literature, some papers reported the theoretical and experimental studies on group III-V and II-VI compounds In 2010, a report on the studies on the electronic, vibrational and thermodynamic properties of ZnS had appeared from M. Cardona, and his group studied [8]. In continuation of the study of zinc-chalcogenides, in 2014, Bilal and his co-workers performed first principle studies of the structural, elastic, electronic and optical properties of Zn-chalcogenides under pressure [9]. In the solid state, the III-V (GaP, GaAs, InP, InAs) and II-VI (ZnS, CdTe, ZnSe) compounds have two common stable structures: zinc-blende (ZB) and rock-salt (RS). These materials in the ZB structure are found to be direct band gap compound, and in the RS structure, they are metallic compound. In this manuscript, the findings of the present work on the typical features of the structural properties and electronic structure of a compound from the group III-V and group II-VI are discussed in detail in the light of density functional (DFT).

II. Computational detail

The zinc-blende and rock-salt structure of the InP and ZnS are generated with the atomic position at (In, Zn: 0.0,0.0,0.0), (P, S: 0.25,0.25,0.25) and (In, Zn: 0.0,0.0,0.0), (P, S: 0.5,0.5,0.5) respectively. All the present calculations are performed using the WIEN2k package developed by P. Blaha, and K. Schwarz *et al*. based on Full Potential Linearized Augmented Plane wave (FP-LAPW) method with LDA, GGA, mBJ-GGA potential as exchange-correlation potentials [10-13]. In this method, the lattice is divided into non-overlapping spheres (called an atomic or muffin tin sphere) surrounding each atomic site and an interstitial region. Therefore, two different types of basis sets are chosen for expressing the single particle wave functions. Inside

the muffin tin region, the basis function is a product of radial function and spherical harmonics. For the interstitial regions that are outside the muffin tin sphere, the basis functions are expanded in plane waves. We perform the initialization, and self-consistent field cycle (SCF). In all the calculations, 20*20*20 k mesh points are used for the integration that reduces to 256 irreducible k-points inside the Brillion zone including five high symmetry points W, L, Γ, X and K. Convergence of the basis set is obtained at $R_{MT}K_{max} = 9.0$ where K_{max} gives us the plane wave cut-off.

III. Result and Discussions

3.1 Structural Properties, the phase transition of InP and ZnS:

Indium phosphide (InP) is the group III-V, and Zinc sulphide (ZnS) is the group II-VI compound that crystallizes both in zinc-blende (space group: 216/F43m) and rock-salt (space group: 225/Fm3m) structure. For the structural optimization, we generate the structure of both the phases of the compounds. We calculate the total energy as a function of the unit cell volume of InP and ZnS as shown in fig.1 (a, b). By fitting the total energy versus unit cell volume to Birch–Murnaghan equation, minimization of the total energy gives the optimized crystal structure [14]. In the figures, the minimum energy (that corresponds to the optimized structure) is found to be lower in case of ZB structure as compared to the RS phase. Thus, we confirm that InP and ZnS in the ZB phase are more stable than their RS phase. The present calculated equilibrium structure parameters such as lattice parameter a_o, bulk modulus B_o, pressure derivative of the bulk modulus $B^/$ are in good agreement with the experimental and theoretical data as given in the table 1 [15-24].
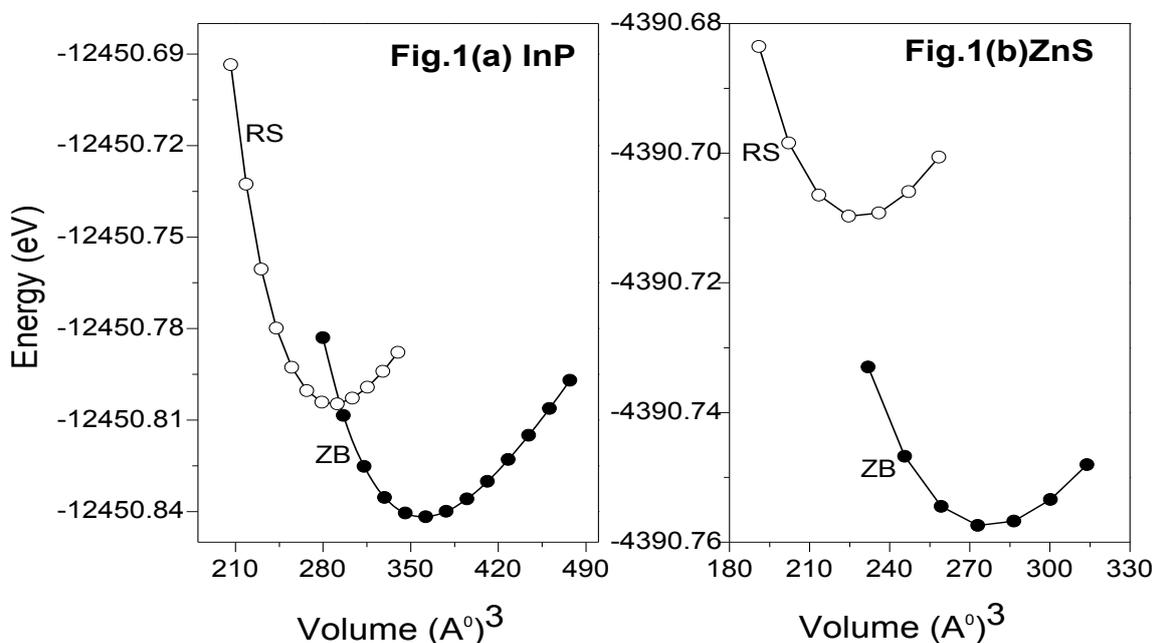
Figure 1: Total energy as a function of unit cell volume of (a) InP (ZB and RS phase) and (b) ZnS (ZB and RS phase).

Table 1: Optimized structure parameters of InP and ZnS in the ZB and the RS structure.

		ZB structure			RS structure			Transition pressure P_t (GPa)
		a_0 (A^0)	B_0 (GPa)	$B^/$	a_0 (A^0)	B_0 (GPa)	$B^/$	
InP	LDA*	5.84	71.93	4.79	5.42	88.61	5.04	6.07
	GGA*	5.97	60.5	4.64	5.54	74.7	4.76	9 .3
	Others work	5.94[15] 5.95[16]	68.0[15]	4.90[15] 4.59[16]	5.71[15] 5.24[16]			9.5[17] 9.8[18]
ZnS	LDA*	5.33	88.88	4.62	5.00	111.75	4.83	15.9
	GGA*	5.47	71.75	4.51	5.14	88.73	4.83	17.6
	Others work	5.41[8] 5.32[19]	76.90[8] 83.80[19]	4.90[8]	5.13[20] 5.06[21]	85.01[22]	4.0[21]	18.1[23], 16.9[24]

*present work
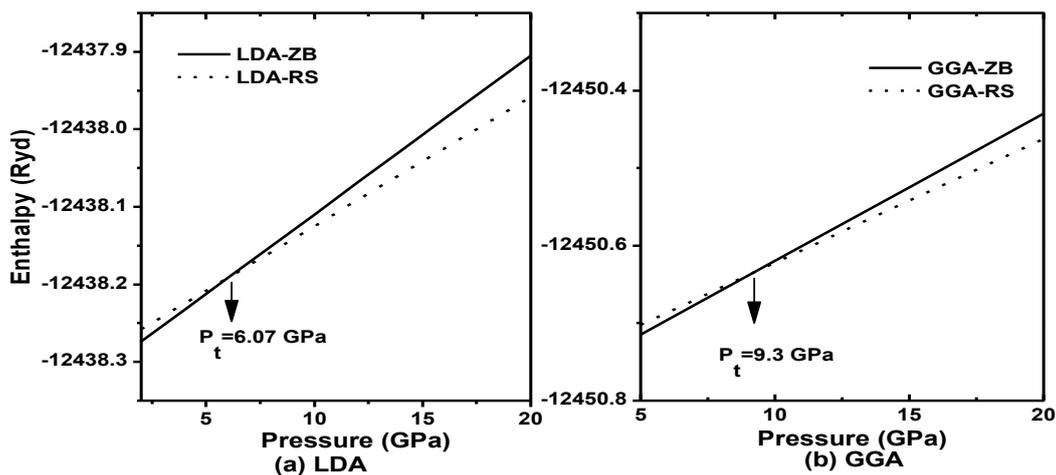
Figure 2: Enthalpy as a function of pressure for InP (ZB and RS phase) with (a) LDA and (b) GGA method.
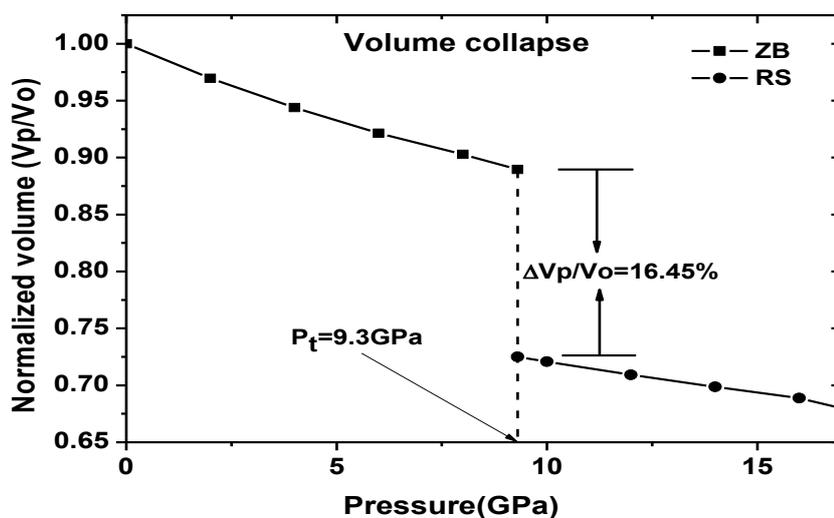
Figure 3: The Normalized volume as a function of pressure for InP (ZB and RS phase).
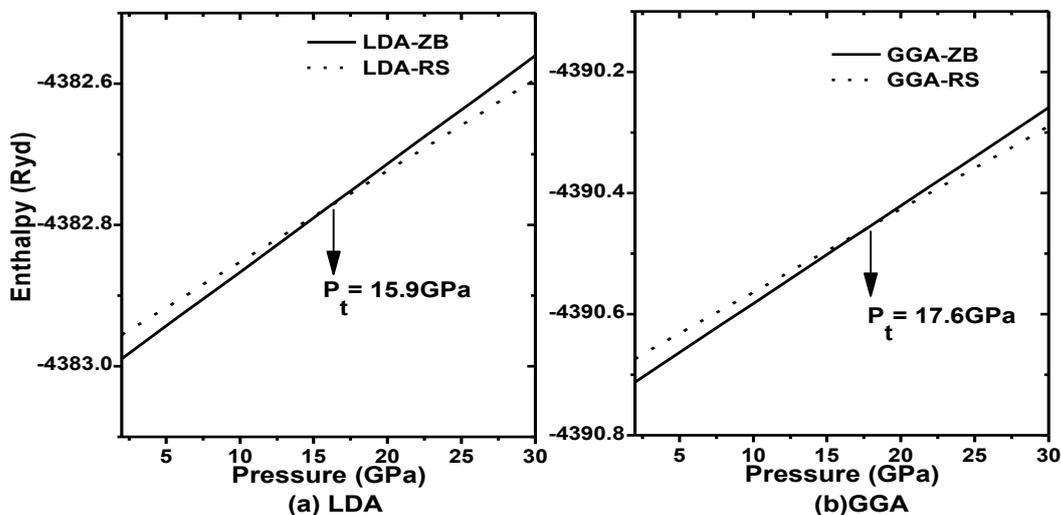
Figure 4: Enthalpy as a function of pressure for ZnS (ZB and RS phase) with (a) LDA and (b) GGA method.
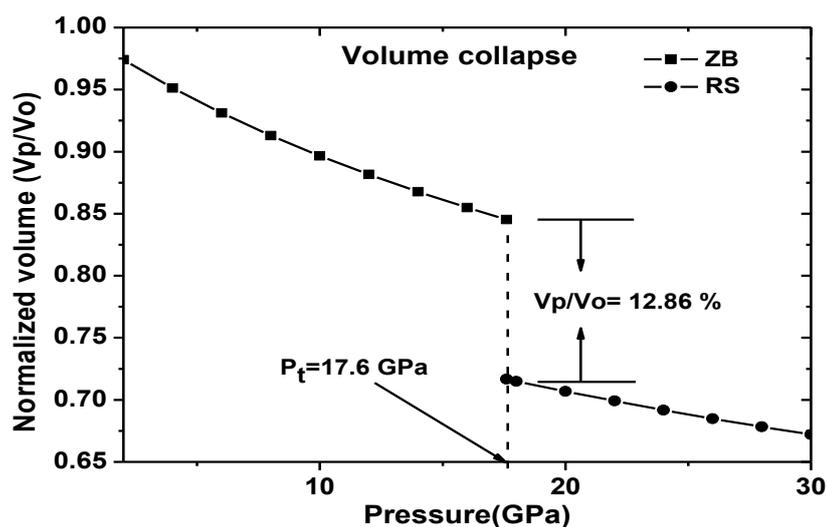
Figure 5: The Normalized volume as a function of pressure for ZnS (ZB and RS phase).

The experimental data available for comparison shows a maximum difference of less than 2% (with GGA method) which is quite acceptable. Thus, we use the present optimized structure for further calculations. Fig.2 shows the enthalpy versus pressure of InP in ZB and RS structure. The pressure at which both the curves are intersected is the transition pressure where structural phase transition takes place. The intersection point is calculated with the least square fitting method. The structural transition of InP (ZB to RS structure) occurs at 6.07 GPa pressure with LDA method and at 9.3 GPa pressure with GGA method. The normalized volume (V_p/V_o) of InP (within GGA) is shown in fig. 3 with a volume decrease of 16.45%. It indicates the ZB phase is more compressible than the RS phase. Also, fig. 4 shows the phase transformation under pressure for ZnS within the LDA calculation, at 15.9 GPa pressure while the transition within the GGA calculation at 17.6 GPa pressure. The volume collapse at the transition is shown in fig. 5 with a volume decrease of 12.86% indicating that the ZB phase is more compressible than the RS phase. A comparison of the results is shown in table 1.

3.2 Electronic structure of InP and ZnS:
Fig. 6 (a, b, c) shows the energy band diagram of InP-ZB phase calculated with (a) LDA, (b) GGA and (c) mBJ-GGA methods. The band diagram in fig. 6(a) with LDA, does not exhibit a clear gap at Γ point, indicating it is metallic nature. However, with GGA method, the gap is seen in the band diagram in fig. 6(b), so it is a semiconductor compound, but this method does not provide correct band gap as experimental value. Thus the LDA and GGA methods give a lower estimate of band gap result; hence GGA-mbj method is used for electronic calculation. The band diagram with GGA-mbj method is shown in Fig. 6(c), the minimum of the conduction band and the maximum of valence band lie in a line at Γ point. Thus InP (in ZB phase) is a direct band gap of 1.31eV in agreement with the experimental result [25]. Fig. 7 shows the band diagram of InP in RS phase with (a) LDA, (b) GGA and (c) mBJ-GGA methods. In all the three methods, the conduction band crosses the Fermi level towards the valence band that concludes InP-RS phase is a metallic compound. We also calculate the electronic structure of other compounds in group III-V such as GaP, GaAs [26,27,28]. The group III-V compounds (crystallized in ZB) phase show direct band gap materials while in RS phase, they exhibit metallic. The total and partial DOS calculations of InP (not given here) show the *s*-orbital of In-atom contributes to the valence band with significant contribution from *p*-orbital of In-atom, *s* & *p*-orbital of P-atom and the *s*-orbital of P-atom contributes mainly to the next lower valence band.
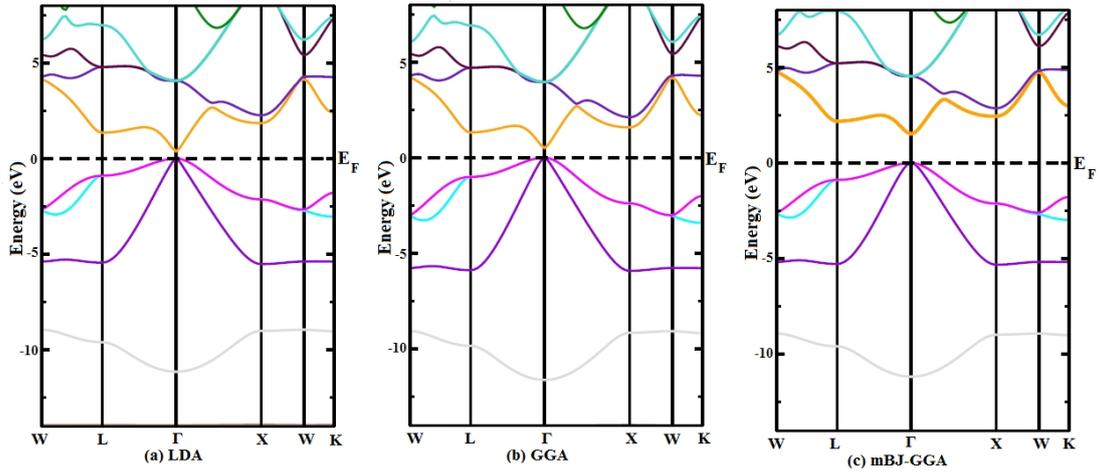
Figure 6: Band structure of InP (ZB phase) at 0 GPa pressure within (a) LDA, (b) GGA and (c) mBJ-GGA method.
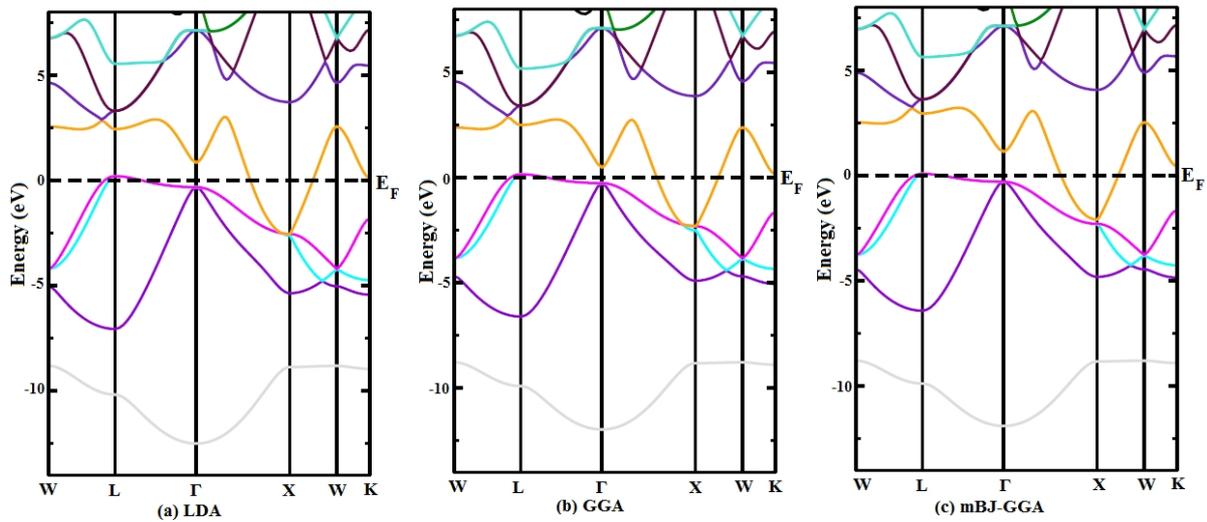
Figure 7: Band structure of InP (RS phase) at 0 GPa pressure within (a) LDA, (b) GGA and (c) mBJ-GGA method.
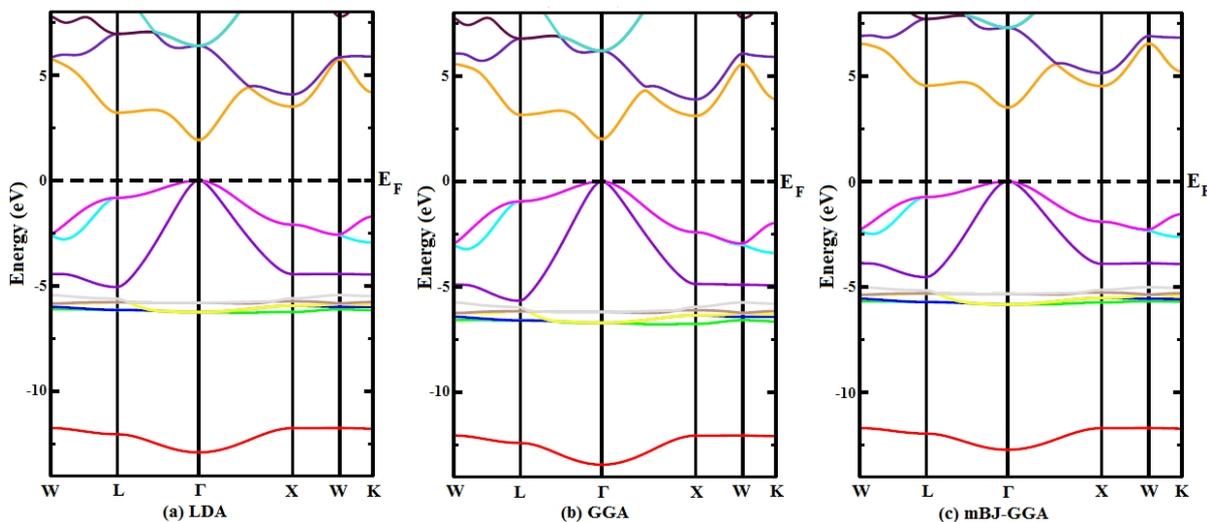
Figure 8: Band structure of ZnS (ZB phase) at 0 GPa pressure within (a) LDA, (b) GGA and (c) mBJ-GGA method.
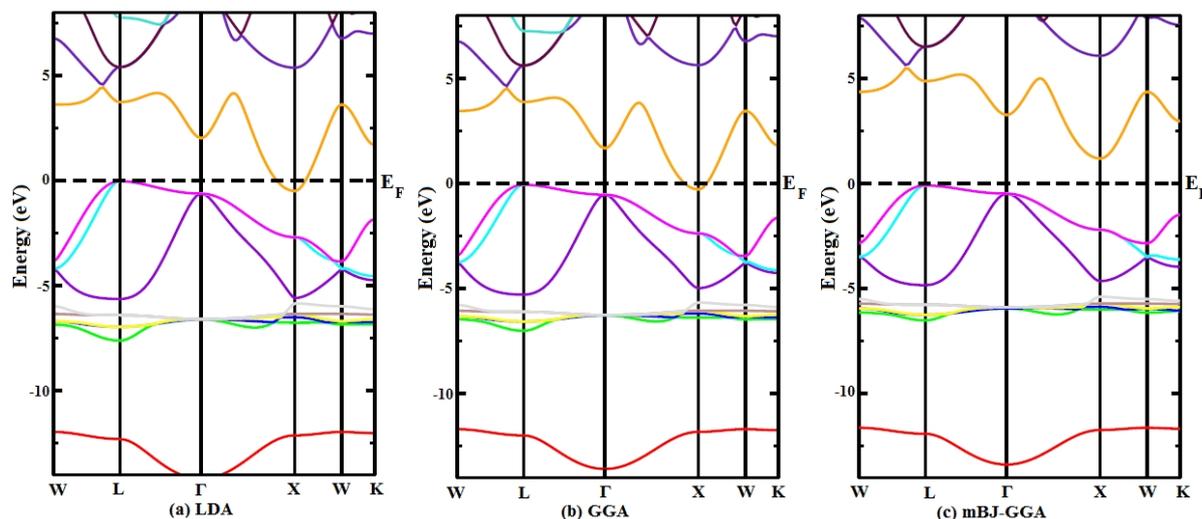
Figure 9: Band structure of ZnS (RS phase) at 0 GPa pressure within (a) LDA,
(b) GGA and (c) mBJ-GGA method.

The energy band diagram of ZnS (in ZB structure) with LDA, GGA, mbj-GGA methods are shown in fig. 8 (a, b, c) and the figures show a direct band gap semiconductor. The band diagram with GGA-mbj in fig. 8(c), shows the band gap at the Γ point as 3.5 eV which is close to the experimental value of 3.6 eV [25]. In the case of the ZnS (in RS structure), the band diagram with LDA, GGA method as shown in fig. 9(a, b) exhibit metallic nature. However, the band diagram in fig. 9(c), with the GGA-mbj method, shows the maximum of valence band lies at L and minimum of conduction band occurs at X symmetry point and thus concludes, an indirect band gap of 1.9 eV. Similar results are also reported in the literature [29,30]. The DOS calculations of ZnS confirm the contribution of *s, p*-orbitals from Zn-atom and S-atom in the energy bands.

IV. Conclusion

The present calculated equilibrium structure parameters of InP (a group III-V compound) and ZnS (a group II-VI compound) are in good agreement with the available experimental and theoretical data. The zinc-blende phase of InP changes its structure to the rock-salt phase under pressure at 9.3 GPa pressure with GGA method which is close to the experimental value with a volume collapse of 16.45% at the transition. In the case of ZnS, the structural phase transition (zinc-blende to rock-salt structure) occurs at 15.9 GPa with a volume collapse of 12.86%. The band diagram of InP (zinc-blende structure) shows a direct band gap of 1.31eV, and metallic in the rock-salt structure. Whereas, the zinc-blende phase of ZnS is a direct band gap compound of 3.5 eV and is an indirect band gap of 1.1eV in its rock-salt phase. The indirect band gap observed in ZnS (rock-salt structure) is a typical feature in agreement with the other reports. The DOS calculations conclude the contributions of the atomic orbital in the energy band diagrams.

References

[1]. A.L. Robinson. GaAs Readied for High-Speed Microcircuits. *Science* **219,** 4582 (275-277) (1983).
[2]. G.D. Pitt, M.K.R. Vyas. Electrical properties of InAs to very high pressures. *Journal of Physics C: Solid State Physics* **6**(2), 274(1973).
[3]. R. Li, Y. Xu, X. Miao, and D. Zhang. Metallic behavior and negative differential resistance properties of (InAs)$_n$ (n=2-4) molecule cluster junctions via a combined non–equilibrium Green's function and density functional theory study. *Journal of Applied Physics* **115**(23), 233712(1-6) (2014).
[4]. W. Fawcett, C. Hilsum, H.D. Rees. Effects of non-parabolicity on non-ohmic transport in InAs. *Solid State Communications* **7**(17), 1257 (1969).
[5]. M. Serra. Structural and electronic properties of narrow-band-gap semiconductors: InP, InAs, and InSb. *Physical Review B* **41**(17), 12079 (1990).
[6]. C.S. Wang, B.M. Klein. First-principles electronic structure of Si, Ge, GaP, GaAs, ZnS, and ZnSe, Self-consistent energy bands, charge densities, and effective masses. *Physical Review B* **24**(6), 3393 (1981).
[7]. S. Massidda, A. Continenza, A.J. Freeman, T.M. De Pascale, F. Meloni, M. Serra. Structural and electronic properties of narrow-band-gap semiconductors: InP, InAs, and InSb. *Physical Review B* **41**(17), 12079 (1990).
[8]. M. Cardona, R.K. Kremer, R. Lauck, G. Siegle, A. Muñoz, A.H. Romero, A. Schindler. Electronic, vibrational, and thermodynamic properties of ZnS with zinc- blende and rocksalt structure. *Physical Review B* **81**(7), 075207(1-13) (2010).
[9]. M. Bilal, M. Shafiq, I. Ahmad, I. Khan. First principle studies of structural, elastic, electronic and optical properties of Zn-chalcogenides under pressure. *Journal of Semiconductors* **35**(7), 072001(1-9) (2014).
[10]. P. Blaha, K. Schwarz, G.K.H. Madsen, D. Kvasnicka, J. Luitz, *WIEN2k An Augmented Plane Wave plus Local Orbitals Program for Calculating Crystal Properties* (Vienna University of Technology, Vienna, Austria, 2001).
[11]. P. Hohenberg W. Kohn. *Physical Review B* **136,** 864 (1964).

[12]. S. Cottenier, *Density Functional Theory and the family of (L)APW-methods: a step-by-step Introduction* (Belgium, 2002).
[13]. J. P. Perdew, S. Burke, M. Ernzerhof. Generalized Gradient Approximation Made Simple. *Physical Review Letters* **77**, 3865 (1996).
[14]. F. Birch. The effect of pressure upon the elastic parameters of isotropic solids according to Murnaghan's theory of finite strain. *Journal of Applied Physics* **9**(4), 279 (1938).
[15]. V.V. Shchennikov, S.V. Ovsyannikov. Thermoelectric properties and phase transitions of II–VI semiconductors at high pressure. *Physica Status Solidi (b)* **244**(1), 437 (2007).
[16]. R.M. Martin. Elastic properties of ZnS structure semiconductors. *Physical Review B* **1**(10), 4005 (1970)**.**
[17]. C.S. Menoni, I.L. Spain. Equation of state of InP to 19 GPa. *Physical Review B* **35**(14), 7520 (1987).
[18]. S. Kalvoda, B. Paulus, P. Fulde, H. Stoll. Influence of electron correlations on ground-state properties of III-V semiconductors. *Physical Review B* **55**(7), 4027 (1997).
[19]. O. Zakharov, A. Rubio, X. Blase, M.L. Cohen, S.G. Louie. Quasiparticle band structures of six II-VI compounds: ZnS, ZnSe, ZnTe, CdS, CdSe, and CdTe. *Physical Review B* **50**(15), 10780 (1994).
[20]. S. Ves, U. Schwarz, N.E. Christensen, K. Syassen, M. Cardona. Cubic ZnS under pressure: Optical-absorption edge, phase transition, and calculated equation of state. *Physical Review B* **42**(14), 9113 (1990).
[21]. H. Cui-E, S. Li-Li, Z. Zhao-Yi, C. Xiang-Rong. Pressure and temperature induced phase transition of ZnS from first-principles calculations. *Chinese Physics Letters* **25**(2), 675(2008).
[22]. S. Lalitha, S. Z. Karazhanov, P. Ravindran, S. Senthilarasu, R. Sathyamoorthy, J. Janabergenov. Electronic structure, structural and optical properties of thermally evaporated CdTe thin films. *Physica B: Condensed Matter* **387**(1), 227 (2007).
[23]. Y. Pan, S. Qu, S. Dong, Q. Cui, W. Zhang, X. Liu, J. Liu, B. Liu, C. Gao, and G. Zou. An investigation on the pressure-induced phase transition of nanocrystalline ZnS. *Journal of Physics: Condensed Matter* **14**(44), 10487 (2002).
[24]. Y. Jun, Z. Feng, Z. Qian, W. Ye, W. Xiang, Q. Shan, D. Jun-Cai, C. Dong-Liang. In situ XAFS investigation on zincblendeZnS up to 31.7 GPa. *Chinese Physics Letters* **30**(4), 046101(1-4) (2013).
[25]. C. Kittel. *Introduction to Solid State Physics*, 6th ed. (Maruzen, Tokyo, 1986).
[26]. Kh. Kabita, Jameson Maibam, B. Indrajit Sharma, R. K. Thapa, R. K. Brojen Singh. Density Functional Theory Study of Electronic Structure, Elastic Properties and Phase Transition of Gallium Phosphide (GaP). *Adv. Sci. Eng. Med.* **6,** 354 (2014).
[27]. Kh. Kabita, Jameson Maibam, B. Indrajit Sharma, R. K. Brojen Singh, R. K. Thapa. Density functional theory study on pressure induced structural transformation, elastic properties and electronic structure of gallium arsenide (GaAs). *International Journal of Innovation and Applied Studies* **8**(1), 382 (2014).
[28]. Kh. Kabita, Jameson Maibam, B. Indrajit Sharma, R. K. Brojen Singh, R. K. Thapa. First principles phase transition, elastic properties and electronic structure calculations of Cadmium Telluride (CdTe) under induced pressure: Density functional theory LDA, GGA and modified Becke Johnson potential. *Materials Research Express* **3,** 15901(1-11) (2016).
[29]. M. Bilal, M. Shafiq, I. Ahmad, I. Khan. First principle studies of structural, elastic, electronic and optical properties of Zn-chalcogenides under pressure. *Journal of Semiconductors* **35**(7), 072001 (1-9) (2014).
[30]. R. Khenata, A. Bouhemadou, M. Sahnoun, et al. Elastic, electronic and optical properties of ZnS, ZnSe and ZnTe under pressure. *Comput Mater Sci* 38(1), 29 (2006).